Published in final edited form as:
J Immunol. 2013 November 15; 191(10): . doi:10.4049/jimmunol.1301490.

Mitochondrial ROS induces NLRP3-dependent lysosomal damage and inflammasome activation[1]

Michelle E. Heid[*], **Peter A. Keyel**[*], **Christelle Kamga**[†], **Sruti Shiva**[†], **Simon C. Watkins**[‡], and **Russell D. Salter**[*]

[*]Department of Immunology, University of Pittsburgh, Pittsburgh, PA, 15261 USA

[†]Department of Pharmacology and Chemical Biology, University of Pittsburgh

[‡]Department of Cell Biology, University of Pittsburgh

Abstract

The NLRP3 inflammasome drives many inflammatory processes and mediates IL-1 family cytokine release. Inflammasome activators typically damage cells, and may release lysosomal and mitochondrial products into the cytosol. Macrophages triggered by the NLRP3 inflammasome activator nigericin show reduced mitochondrial function and decreased cellular ATP. Release of mitochondrial ROS leads to subsequent lysosomal membrane permeabilization (LMP). NLRP3-deficient macrophages show comparable reduced mitochondrial function and ATP loss, but maintain lysosomal acidity, demonstrating that LMP is NLRP3 dependent. A subset of WT macrophages undergo subsequent mitochondrial membrane permeabilization (MMP) and die. Both LMP and MMP are inhibited by potassium, scavenging mitochondrial ROS, or NLRP3 deficiency, but are unaffected by cathepsin B or caspase-1 inhibitors. In contrast, IL-1β secretion is ablated by potassium, scavenging mitochondrial ROS, and both cathepsin B and caspase-1 inhibition. These results demonstrate interplay between lysosomes and mitochondria that sustain NLRP3 activation, and distinguish cell death from IL-1β release.

Introduction

Inflammasome activation plays an integral part of the innate immune response in host defense and in other inflammatory diseases. The NOD-like receptor family, pyrin domain-containing three (NLRP3) inflammasome is present in a variety of cells, including macrophages, dendritic cells, neutrophils, T cells, B cells, and some epithelial cells (1). The NLRP3 inflammasome is a protein scaffolding complex consisting of NLRP3, caspase-1, and the adaptor molecule ASC (Pycard) that induces secretion of IL-1 family cytokines, including interleukin-18 (IL-18) and interleukin-1 beta (IL-1β) (2, 3). The processing of IL-1β from biologically inactive precursor to the active form requires cleavage by caspase-1, which is recruited to the NLRP3 inflammasome complex by binding ASC. In addition, NLRP3 activation triggers an inflammatory caspase-1 dependent death process termed pyroptosis (4). While IL-1β processing and release require caspase-1 catalytic activity, pyroptosis can be mediated by uncleaved caspase-1 following activation of NLRC4 or AIM2 inflammasomes (5).

[1]This work was funded by NIH grants T32AI089443, T32AI060525, and 5R01AI072083. The work at the Center for Biological Imaging was funded by the NIH grant P30CA47904.

Corresponding author: Russell D. Salter, 200 Lothrop Street, Pittsburgh, PA 15261, phone: 412-648-9471, fax: 412-383-8096, rds@pitt.edu.

The authors declare no conflict of interest.

While the exact mechanism of NLRP3 inflammasome activation has remained elusive, a variety of danger associated molecular patterns and pathogen associated molecular patterns, including ATP, nigericin, pore forming toxins, silica crystals, and alum have been shown to trigger inflammation through NLRP3 activation (6). The chemical diversity of these stimuli suggests that they may induce a common cellular stress response rather than binding directly to the NLRP3 inflammasome. Potassium efflux from cells is required for NLRP3 activation by almost all stimuli examined, suggesting that compromised membrane integrity is a common feature of this pathway (1).

Several reports attributed the activation of the NLRP3 inflammasome to the leakage of lysosomal contents into the cytosol following phagocytosis of particulate stimuli that could damage their integrity (7, 8). Using inhibitors that blocked inflammasome activation, it was suggested that cathepsin B might be responsible for proteolytically activating NLRP3 inflammasome (7). This process, characterized by the loss of lysosomal contents and acidity, has been termed lysosomal membrane permeability (LMP) (9). There remains uncertainty about the generality of this model since not all NLRP3 activators are phagocytosed and disrupt lysosomes directly. Further, it has been suggested that the cathepsin B inhibitor used, CA-074 Me, may not be specific, as RNAi knockdown and use of cells from cathepsin $B^{-/-}$ mice did not recapitulate CA-074 Me results (9, 10). Alternatively, release of reactive oxygen species (ROS) into the cytosol during LMP could trigger NLRP3 activation, suggested by the observation that NLRP3 inflammasome can be activated by addition of superoxide to macrophage cultures (11). However, inhibition of lysosomal ROS generation with Nox1-4 knockout mice did not show a corresponding decrease in NLRP3 inflammasome activation (11, 12).

A role for mitochondria as another potential source of ROS has also been explored (11, 13). Mitochondria are sensitive to cellular stress, and respond through depolarization of the mitochondrial membrane, ROS release, a decrease in mitochondrial ATP, and reversible opening of the mitochondrial permeability transition pore. A later marker of mitochondrial damage, mitochondria membrane permeability (MMP), can result in the release of additional mitochondrial contents, including cytochrome c, and eventual cell death (14, 15).

Recent reports showing that mitochondrial DNA (mtDNA) can activate the NLRP3 inflammasome have further supported a role for mitochondria in inflammasome activation (16). Inhibition of mitophagy promotes the accumulation of dysfunctional mitochondria in cells, and their eventual breakdown was suggested to increase levels of mtDNA in the cytosol (17). A second study showed directly that oxidized mtDNA can activate NLRP3 inflammasome (18).

Here, we present evidence that NLRP3 inflammasome activation occurs prior to both LMP and MMP. Using a combination of live cell imaging and biochemical approaches, we demonstrate that prototypical NLRP3 stimuli, the potassium ionophore nigericin, or millimolar concentrations of ATP, exert both NLRP3 independent and dependent effects on macrophages that result in cytokine release and cell death. We present a kinetic model integrating the roles of mitochondria and lysosomes in this process.

Materials and Methods

BMDM preparation

As previously described (19), bone marrow was harvested from the tibiae and femora of WT or $NLRP3^{-/-}$ B6 mice (gifts from Dr. Lisa Borghesi, Dr. Olivera Finn, and Dr. Timothy Billiar). Cells were grown in the presence of 20% FBS (Gemcell), 2 mM L-glutamine (Cellgro), 500 U penicillin/500 μg streptomycin (Lonza), 1 mM sodium pyruvate (MP

Biomedicals), and 30% L cell supernatant made from culturing L cell fibroblasts (CCL-1 from American Type Culture Collection) for about six days. Media of monocytes was replaced after four days. Cells were then harvested and grown in IMDM (HyClone), called cIMDM when supplemented with 10% FBS, 2 mM L-glutamine, 500 U penicillin/500 μg streptomycin and were harvested with Cellstripper (Cellgro) for experiments from day 8–25.

TLO Preparation

Tetanolysin O (Enzo) was reduced as previously described (19). Serum containing media was washed out prior to the addition of TLO to cells. 100 ng/ml was added in serum free media to appropriate dishes and incubated at 37°C for the duration of imaging as indicated.

MTT assay

WT or NLRP3$^{-/-}$ BMDM were plated the day before the experiment at 500,000 cells/well in a 12 well tissue culture plate (Costar) in cIMDM, as described above. Cells were incubated for 4 hours with 1 μg/ml LPS (Sigma). 50 mM KCl, 100 μM or 500 μM MitoTEMPO (Enzo), or 100 μM Ac-YVAD-CMK (Alexis) were added during the last 30 minutes of LPS treatment and then re-added when media was removed and 1ml fresh phenol red-free supplemented IMDM (Gibco) was added to the wells. 20 μM of nigericin sodium salt (Sigma) or 30 mM ATP (Sigma) was added to the wells and incubated at 37°C for 5–30 minutes. After supernatants were removed, cells were washed once with 1× DPBS (Cellgro) and the Vybrant® MTT cell proliferation assay kit (Invitrogen/Molecular Probes) was used according to the manufacturer's instructions. Samples were then assayed in duplicate for OD using a PowerWave XS microplate spectrophotometer. Percent MTT converted to formazan in the sample was calculated by (mean OD of sample-mean OD of blank)/(mean OD of untreated control- mean OD of blank) X 100. Percent unconverted MTT was graphed.

LDH Release Assay

WT and NLRP3−/− BMDM were treated as described above for the MTT assay. 1% Triton X-100 (Fisher Scientific) was incubated with cells for five minutes as a positive control for complete cell lysis. Supernatants were removed and assayed in duplicate using an LDH cytotoxicity kit (Cayman Chemical) for OD using a PowerWave XS microplate spectrophotometer (BioTek). Percent LDH release was calculated as (mean OD value of sample-mean OD value of blank)/(mean OD value of TritonX-100 control sample – mean OD of blank) X100.

Quantification of ATP remaining in cell

WT or NLRP3$^{-/-}$BMDM were treated as described for the LDH assay. Supernatants were removed. Using CellTiter-Glo Luminescent Cell Viability Assay (Promega), ATP levels remaining in the cell lysates were determined using a Berthold Orion microplate luminometer according to the kit instructions and Simplicity 2.1 software. Results were recorded as a percentage of ATP remaining in cells based on untreated control cells.

Seahorse Assay

WT or NLRP3$^{-/-}$ BMDM were plated the night before at 500,000 cells/well in a Seahorse 24 well V7 microplate. Cells were LPS primed at 1 μg/ml for four hours. Media was removed from wells and cells were incubated in buffered growth media for an hour after pre-treatment with nitrite. 20 μM nigericin was added into wells in unbuffered media prior to inserting plate into Seahorse XF24 Extracellular Flux analyzer (Seahorse Bioscience). After 21.5 minutes of equilibration, media was injected as a control, oligomycin (20 μM) was injected into each well at 48 minutes, followed by FCCP (75 μM) at 73 minutes, and

rotenone (20 μM) at 99 minutes. OCR was recorded as pMoles/min. Averages of three wells were taken per data point.

Live cell microscopy

WT or NLRP3$^{-/-}$ BMDM were plated at 250,000 cells/dish in 35 mm collagen coated glass bottom culture dishes (MatTek) the night before the experiment in cIMDM. Media was removed and cells were LPS primed (1 μg/ml) for three to four hours in fresh media. Inhibitors were added during the last 30 minutes of LPS priming at 37°C and were added back to the dish in fresh media before imaging, following washing out LPS containing media. YVAD was added at 100 μM, CA-O74 Me (Calbiochem) was added at 100 μM. 2μM MitoTracker Red CM-H2XRos (Invitrogen), 10 μM TMRM, or 2 μM LysoTracker Green DND-26 (Invitrogen) were added during the last 30 minutes of LPS priming. 10 μl/ml pSIVA (Imgenex) was added in 1 ml of complete IMDM two frames after the initiation of imaging after 30 minutes pre-incubation. Dishes were imaged on Nikon A1 inverted microscope with a Plan Fluor 40× objective with an 1.30 NA or Plan Apo 60× objective with an 1.40 NA, Photometrics Coolsnap HQ2 or Andor™ Technology iXon^{EM} + camera, NikonPiezo driven XYZ stage, and Tokai Hit Environmental chamber. For MitoTracker, LysoTracker, TMRM, and pSIVA, images were captured every 30 seconds for one hour. 20 μM nigericin or 3 mM ATP was added 2 minutes into imaging in 1ml of media. Videos were analyzed using Elements (Nikon) and Microsoft Excel.

IL-1β ELISA

WT or NLRP3$^{-/-}$ BMDM were plated at 500,000 cells/well in a 12 well tissue culture plate the night before. Cells were LPS primed for four hours and treated as indicated. An IL-1β ELISA was performed as previously described (19). OD values were read at 450 nm with 570 nm background subtraction using BioTek® Powerwave XS Microplate Spectrophotometer and Gen5^{TM} Data Analysis Software.

IL-1β Western Blot

Lysates and supernatants were collected from 2.0 × 10^6 BMDM after treating cells as indicated in serum-free IMDM. Supernatants were TCA precipitated and both lysates and supernatants were analyzed for IL-β via Western blot as previously described (19). Western blotting luminal reagent (Santa Cruz) was added before imaging on a Kodak Image Station 4000MM (Molecular Imaging Systems).

Statistical analysis

All data sets were analyzed via a student's two-tailed t-test unless otherwise noted using Graphpad software. P values were as indicated and were considered significant if $P<0.05$.

Results

NLRP3 inflammasome activation increases sensitivity of bone marrow derived macrophages to membrane damage

The NLRP3 inflammasome is present in a variety of immune cells, including macrophages. Due to the robustness of NLRP3 activation in murine bone marrow derived macrophages (BMDM), this system has frequently been employed to examine NLRP3 inflammasome activation and function. BMDM were primed with LPS for three to four hours to up-regulate inflammasome components as well as induce the translation of pro-IL-1β, a cytokine that is processed into its active form during NLRP3 inflammasome dependent caspase-1 activation. Following priming, BMDM from wild type C57/BL6 mice were treated with the potassium ionophore nigericin, a prototypical activator of the NLRP3 inflammasome.

To test membrane permeability, lactate dehydrogenase (LDH) was measured in the culture supernatants. Following nigericin treatment, LDH levels were increased in the supernatants of LPS primed wild type BMDM but not LPS primed NLRP3$^{-/-}$ cells, indicating that the cell membrane integrity had been compromised in the former (Figure 1A). Pre-treatment of WT BMDM with 50 mM KCl to block potassium efflux significantly inhibited release of LDH. Non-LPS primed or BMDM treated with LPS alone did not release LDH above background levels.

An additional assay of cell viability, the conversion of MTT to formazan, which is carried out by mitochondrial reductases, showed similar results. LPS-primed WT and NLRP3 $^{-/-}$ BMDM differed significantly in MTT reduction after nigericin exposure (Figure 1B). We next tested whether ATP, a second well characterized stimulator of NLRP3 inflammasome, promoted similar responses. As with nigericin, 3mM ATP treatment resulted in an inflammasome dependent reduction of MTT conversion to formazan. Together, these results demonstrate that the NLRP3 inflammasome mediates membrane damage.

Nigericin alters mitochondrial function independently of NLRP3

To explore how inflammasome activating stimuli impact mitochondrial function, we measured ATP levels in LPS primed BMDM following nigericin exposure. Both WT and NLRP3$^{-/-}$ BMDM treated with nigericin contained reduced amounts of ATP compared to non-nigericin treated cells, suggesting either decreased synthesis, increased consumption, or release of ATP into the culture supernatant (Figure 2A). ATP levels in nigericin treated cells were not preserved by co-exposure to KCl, consistent with a NLRP3-independent event.

To further characterize nigericin-induced alterations in mitochondrial function, we used the Seahorse assay to measure oxygen consumption rate (OCR) in WT and NLRP3$^{-/-}$ BMDM. Basal OCR levels in non-primed WT and NLRP3$^{-/-}$ BMDM were comparable, while both showed reduced OCR levels four hours after LPS priming. Nigericin rapidly increased OCR levels in both LPS primed WT and LPS primed NLRP3$^{-/-}$ BMDM, indicating a stress response in mitochondrial respiration (Figures 2B and 2C). Following nigericin exposure, cells from both cell types were unable to respond to oligomycin or FCCP, which respectively inhibit ATP synthesis and uncouple electron transport. In contrast, LPS primed WT or NLRP3$^{-/-}$ BMDM decreased OCR in response to oligomycin, followed by increased OCR in response to FCCP, which could be blocked by rotenone. These data show that LPS priming and nigericin each disrupt mitochondrial respiration in BMDM independently of NLRP3, with more severe dysfunction occurring after nigericin treatment. Taken together, these data demonstrate that nigericin reduces OCR and diminishes cellular ATP levels independently of NLRP3 in BMDM.

Loss of mitochondrial membrane integrity and cell death are NLRP3 dependent

Since WT and NLRP3$^{-/-}$ BMDM differ greatly in their ability to convert MTT through mitochondrial reductases (Fig 1B), we further probed potential effects of NLRP3 on mitochondria using MitoTracker Red to measure membrane integrity. Using live cell microscopy, we found that nigericin- or ATP- treated, LPS primed WT and NLRP3$^{-/-}$ BMDM showed distinct differences in mitochondrial integrity (Figures 3A– C, and Supplementary Videos 1 and 2). Approximately 30% of WT BMDM exhibited complete loss of mitochondrial integrity, while no loss was detected in NLRP3$^{-/-}$ BMDM in one hour (Figure 3D). In LPS primed untreated or non-primed nigericin treated BMDM, no loss of mitochondrial integrity was seen (Figures 3B,C). Furthermore, both nigericin and ATP induced MMP could be significantly reduced with exposure to KCl (Figure S1A). Loss of mitochondrial membrane integrity correlated with exposure of phosphatidylserine (PS) at the plasma membrane (Figures 3A and 3D). PS exposure was inhibited by the addition of

KCl (Figure 3E). These data demonstrate that NLRP3 inflammasome increases sensitivity of BMDM to loss of mitochondrial membrane integrity and subsequent cell death.

We investigated mtDNA localization in cells using PicoGreen, a dsDNA specific dye which labels mitochondria and nuclei (20). We observed a decrease in mitochondrial PicoGreen staining in LPS-primed WT BMDM, but not in NLRP3$^{-/-}$ BMDM after 1h exposure to nigericin (Supplementary Video 3 and 4). Loss of mtDNA in WT cells was prevented by KCl (data not shown), and coincided with loss of MitoTracker Red (Supplementary Video 3).

Lysosomal membrane permeabilization precedes mitochondrial integrity breakdown during NLRP3 activation

A previously proposed model for NLRP3 activation suggested that following phagocytic uptake of indigestible particles known to trigger IL-1β secretion, rupture of phagolysosomes would release proteases into the cytosol leading to assembly and activation of the NLRP3 inflammasome (7). We evaluated one aspect of this model using live cell imaging. Lysosomes labeled with Lysotracker Green lose fluorescence within 15 min after exposure to nigericin in LPS-primed WT cells (Figure 4A), consistent with either loss of lysosomal acidity or a loss of lysosomal membrane integrity in a process termed LMP. Labeled lysosomes in NLRP3$^{-/-}$ BMDM however retained fluorescence after nigericin treatment, demonstrating that LMP is NLRP3 dependent. LMP was also induced in WT, but not NLRP3$^{-/-}$ BMDM, by two other NLRP3 inflammasome activators, the pore forming toxin tetanolysin O (TLO) (Figure S1 B) and ATP (and data not shown). LMP always preceded MMP in both nigericin and ATP treated WT BMDM (Figure 4B). In nigericin treated cells, LMP occurred within 15 minutes of exposure to the stimulus, while MMP typically required between 30–60 min. In ATP treated cells, LMP occurred within 10 minutes of exposure to the stimulus and MMP typically required 15 to 30 min. In addition, all WT BMDM exposed to nigericin underwent LMP, while on average no more than 60–70% underwent MMP within 60 min (Figure 4C). In contrast, NLRP3$^{-/-}$ BMDM did not undergo LMP or MMP with the 60 min experiment. LMP was blocked in WT BMDM by KCl, consistent with NLRP3 dependence of the process (Figure S1 C). Our results demonstrate that NLRP3 inflammasome activation results in loss of membrane integrity in lysosomes and mitochondria in kinetically distinct events.

IL-1β processing and secretion kinetically precedes loss of mitochondrial membrane integrity

A major function of the NLRP3 inflammasome in immunity is to regulate secretion of a family of non-conventionally secreted cytokines, including IL-1β. To probe the role of mitochondria and lysosomes in cytokine secretion, we performed kinetic analysis of processed IL-1β secretion. Processed IL-1β was detected in the supernatants of LPS primed WT BMDM 15 minutes after nigericin exposure, and levels continued to increase over thirty minutes of nigericin exposure (Figure 5A). Similar kinetics of IL-1β secretion were observed in LPS primed ATP treated WT BMDM (data not shown). Western blotting was used to confirm that released IL-1β was the cleaved biologically active form, not unprocessed precursor (Figure S2). IL-1β release was significantly decreased by addition of KCl five minutes after nigericin exposure, with progressively less inhibition occurring with KCl added at later times within the 30 min nigericin incubation period (Figure 5B). Since LPS primed, nigericin exposed BMDM lose mitochondrial integrity and expose plasma membrane PS by about 30 minutes (Figures 3 and 4), this suggests that IL-1β secretion precedes cell death and MMP, and correlates kinetically with LMP. LDH release occurred with nearly identical kinetics to IL-1β secretion and was also inhibited by KCl, consistent with compromised plasma membrane integrity before cell death (Figures 5C–D).

IL-1β secretion distinct from organelle damage and cell death

To characterize the mechanisms underlying MMP, LMP, and IL-1β processing and secretion, we examined the requirement for caspase-1 in each process. Ac-YVAD-cmk (YVAD), a caspase-1 inhibitor, did not prevent the loss of lysosomal membrane integrity or mitochondrial membrane integrity in WT BMDM treated with nigericin (Figure 6A). Furthermore, YVAD pre-treatment blocked processing and secretion of IL-1β but did not significantly inhibit LDH release from WT BMDM (Figures 6B and 6C). While caspase-1 activity is required for the processing and secretion of mature IL-1β, it does not appear to be required in its active form to trigger LMP, MMP, or cell death.

We and others have shown the cathepsin B inhibitor, CA-074 Me, inhibits secretion of processed IL-1β (7, 19). Cathepsin B is a lysosomal protease that is likely released during LMP. Since processing and secretion of IL-1β correlates kinetically with LMP (Figures 4 and 5), we tested whether cathepsin B participates in MMP. CA-074 Me did not inhibit LMP or MMP induced by nigericin in LPS primed BMDM (Figure S3 A). These results show that the role of NLRP3 inflammasome in IL-1β processing and secretion is distinct from effects on lysosomal and mitochondrial membrane integrity in its dependence on caspase-1 and cathepsin B.

NLRP3 dependent organelle damage and cytokine release is mediated by mitochondrial ROS

Next we examined the potential role for mitochondrial ROS in IL-1β processing and secretion, LDH release, LMP, and MMP. MitoTEMPO, a mitochondria specific ROS scavenger, reduced both IL-1β secretion after nigericin or ATP exposure (Figure 6B) and LDH release after nigericin exposure in LPS primed WT BMDM (Figure 6C) (17). In addition, 500 μM MitoTEMPO also delayed LMP and reduced subsequent MMP in nigericin treated WT BMDM (Figures 6D and 6E and Supplemental Table I). Furthermore, LMP was significantly delayed and MMP reduced when ATP exposed WT BMBM were treated MitoTEMPO (Figure 6E and Figure S3 B). Together, these data suggest that mitochondrial ROS production is an early event that may lead to NLRP3 activation, as well as inflammasome dependent LMP, IL-1β secretion, MMP, and cell death.

Discussion

Our results show that in addition to mediating processing and secretion of inflammatory cytokines, NLRP3 inflammasome influences the function and integrity of organelles, cell membrane permeability, and cell death. We examined the kinetics of these events at the single cell level using live cell microscopy in combination with biochemical assays in macrophages exposed to a prototypical NLRP3 activating stimulus. Our data suggest a multi-step process of mitochondrial and lysosomal dysfunction and damage. Nigericin induces mitochondrial dysfunction and loss of cellular ATP independently of NLRP3 expression. The loss of cellular ATP was unaffected by addition of exogenous KCl, further supporting their NLRP3 independence. In WT but not NLRP3 deficient cells, lysosomal deacidification is observed and followed kinetically by loss of mitochondrial integrity (MMP) and exposure of PS on the cell surface. ROS derived from mitochondria appear to be responsible at least in part for the observed effects on lysosomes, termed lysosomal membrane permeability (LMP), since the ROS scavenger MitoTempo can delay both LMP and inhibit subsequent MMP. Both LMP and MMP can be inhibited in WT cells by exogenous KCl, which prevents the K^+ efflux required for NLRP3 activation. Based on these results in both nigericin treated and ATP treated cells, we propose a model in which some NLRP3 inflammasome activators induce mitochondrial and lysosomal damage, releasing soluble factors from these organelles that sequentially perpetuate inflammasome

activation and cell damage. Although the exact kinetics of these events differ between NLRP3 inflammasome activators, our data with two distinct stimuli suggest the sequence of events may remain the same. Our data strongly support a role for mitochondrial ROS released into the cytosol as one of these mediators, acting to induce LMP.

Inflammasome-mediated cell death is important for removal of cells infected with intracellular pathogens such as Salmonella (21). However, the most widely recognized functions of inflammasomes are to mediate extracellular release of IL-1 cytokine family members. While we and others have been unable to visualize release of these cytokines from individual cells, IL-1β release can be detected in culture supernatants from WT cells by 15 min after nigericin exposure, which closely matches when LMP is first detected in nigericin treated cells. This supports, but does not prove, a role for LMP in IL-1β secretion. Our data do not exclude the possibility that LMP could increase IL-1β release by inducing additional ROS release from mitochondria, and further amplifying the cross-talk pathway with lysosomes (22). We found that when mitochondrial ROS production was inhibited with MitoTEMPO, both LMP and IL-1β secretion were reduced in ATP and nigericin treated cells. In contrast, we do not observe MMP and PS exposure in any cells until after IL-1β is readily detectable in culture supernatants, consistent with IL-1β release not requiring cell death.

Since LMP precedes MMP, it could be suggested that released lysosomal products directly damage mitochondria, resulting ultimately in cell death (15, 23). The identity of products from lysosomes that could destabilize mitochondria is unclear, but might be suggested to include ROS generated by NADPH oxidases (NOXs) in lysosomes, based on results reported in tumor cells (24). However, Nox1-4 deficient macrophages have been shown to produce normal levels of IL-1β, suggesting that lysosomal ROS is not required for NLRP3 inflammasome dependent cytokine release (25, 26). An additional lysosomal product that might induce mitochondrial dysfunction is cathepsin B (27), which has been suggested to participate in NLRP3 inflammasome activation after its release from lysosomes into the cytosol in response to particulate inflammasome stimuli (7). Our data place NLRP3 activation upstream of LMP, which is inconsistent with this hypothesis, unless cathepsin B can be released from intact lysosomes. While able to block IL-1β secretion, the cathepsin B inhibitor CA-074 Me had no effect on MMP. In summary, our data do not support a role for lysosomal products in inducing MMP, but do not exclude this possibility.

An important question raised by our experiments is how mitochondria and their products, including but not limited to ROS, can induce LMP in an NLRP3-dependent fashion. One possibility is suggested by a recent study showing that NLRP3 protein localized in the ER assembles with ASC bound to mitochondria, and that this is mediated through microtubule based movement of mitochondria (28). NLRP3 assembly might thus alter the distribution of mitochondria in the cell, bringing them into proximity with lysosomes, which can also be transported via microtubules (29). Lysosomes in WT but not NLRP3 deficient cells might then encounter higher concentrations of mitochondrial ROS or other released products, leading to selective damage and LMP.

In addition to ROS, mitochondrial DNA has been shown to activate the NLRP3 inflammasome (17). When we labeled mtDNA in BMDM with PicoGreen, we observed loss of signal from mitochondria in WT cells but no signal loss in NLRP3 deficient BMDM. The kinetics were identical to those seen for loss of MitoTracker Red in nigericin treated cells, consistent with loss of mtDNA during MMP. This suggests that mtDNA is released from mitochondria largely after NLRP3 inflammasome is activated, although it does not exclude the possibility that small amounts of mtDNA could be released during initial mitochondrial dysfunction.

Our results show that both LMP and MMP in BMDM do not require active caspase-1, since they each are unaffected by the inhibitor YVAD. We have conducted preliminary experiments with BMDM from caspase-1 deficient mice and see partial inhibition of MMP. However, these mice also lack caspase-11, which plays a role in cell death, clouding interpretation of this data (30–32). Since YVAD blocks caspase-1 cleavage, uncleaved caspase-1 could potentially mediate cell death, as shown for AIM2 and NLRC4 inflammasomes (5). However, NLRP3 lacks the CARD domain needed to directly recruit uncleaved caspase-1.

NLRP3 inflammasome assembles at the ER-mitochondrial interface (28, 33) the site where autophagosomes have been recently shown to form in non-immune cells (34). Inhibition of autophagy or mitochondrial autophagy (mitophagy) have been shown to increase IL-1β secretion in macrophages, perhaps through the accumulation of damaged mitochondria leading to elevation of cytosolic ROS levels (35–37). While precisely how IL-1 family cytokines are packaged for secretion remains unclear, we speculate that autophagy might interfere with packaging of IL-1β into specialized secretory vesicles also originating from this site.

Supplementary Material

Refer to Web version on PubMed Central for supplementary material.

Acknowledgments

We would like to thank the present and past members of the Salter lab, especially Jessica Chu, L. Michael Thomas, and Chengqun Sun. WT or NLRP3$^{-/-}$ bone marrow was provided by Lisa Borghesi, Timothy Billiar, Olivera Finn, Robert Binder, Gabriel Nuñez, and Richard Flavell (Howard Hughes Medical Institute). The Center for Biological Imaging provided reagents, technical support, and advice, especially Greg Gibson and Salony Maniar. We would like to thank the laboratory of Lawrence Kane for the use of their luminometer. Catherine Corey provided technical assistance with the Seahorse assay.

References

1. Petrilli V, Dostert C, Muruve DA, Tschopp J. The inflammasome: a danger sensing complex triggering innate immunity. Curr Opin Immunol. 2007; 19:615–622. [PubMed: 17977705]
2. Agostini L, Martinon F, Burns K, McDermott MF, Hawkins PN, Tschopp J. NALP3 forms an IL-1beta-processing inflammasome with increased activity in Muckle-Wells autoinflammatory disorder. Immunity. 2004; 20:319–325. [PubMed: 15030775]
3. Dubyak GR. P2X7 receptor regulation of non-classical secretion from immune effector cells. Cell Microbiol. 2012; 14:1697–1706. [PubMed: 22882764]
4. Miao EA, Rajan JV, Aderem A. Caspase-1-induced pyroptotic cell death. Immunol Rev. 2011; 243:206–214. [PubMed: 21884178]
5. Broz P, von Moltke J, Jones JW, Vance RE, Monack DM. Differential requirement for Caspase-1 autoproteolysis in pathogen-induced cell death and cytokine processing. Cell Host Microbe. 2010; 8:471–483. [PubMed: 21147462]
6. Bauernfeind F, Ablasser A, Bartok E, Kim S, Schmid-Burgk J, Cavlar T, Hornung V. Inflammasomes: current understanding and open questions. Cell Mol Life Sci. 2011; 68:765–783. [PubMed: 21072676]
7. Hornung V, Bauernfeind F, Halle A, Samstad EO, Kono H, Rock KL, Fitzgerald KA, Latz E. Silica crystals and aluminum salts activate the NALP3 inflammasome through phagosomal destabilization. Nat Immunol. 2008; 9:847–856. [PubMed: 18604214]
8. Halle A, Hornung V, Petzold GC, Stewart CR, Monks BG, Reinheckel T, Fitzgerald KA, Latz E, Moore KJ, Golenbock DT. The NALP3 inflammasome is involved in the innate immune response to amyloid-beta. Nat Immunol. 2008; 9:857–865. [PubMed: 18604209]

9. Newman ZL, Leppla SH, Moayeri M. CA-074Me protection against anthrax lethal toxin. Infect Immun. 2009; 77:4327–4336. [PubMed: 19635822]
10. Dostert C, Guarda G, Romero JF, Menu P, Gross O, Tardivel A, Suva ML, Stehle JC, Kopf M, Stamenkovic I, Corradin G, Tschopp J. Malarial hemozoin is a Nalp3 inflammasome activating danger signal. PLoS One. 2009; 4:e6510. [PubMed: 19652710]
11. Zhou R, Tardivel A, Thorens B, Choi I, Tschopp J. Thioredoxin-interacting protein links oxidative stress to inflammasome activation. Nat Immunol. 2010; 11:136–140. [PubMed: 20023662]
12. Latz E. NOX-free inflammasome activation. Blood. 2010; 116:1393–1394. [PubMed: 20813905]
13. Sorbara MT, Girardin SE. Mitochondrial ROS fuel the inflammasome. Cell Res. 2011; 21:558–560. [PubMed: 21283134]
14. Green DR, Kroemer G. The pathophysiology of mitochondrial cell death. Science. 2004; 305:626–629. [PubMed: 15286356]
15. Boya P, Andreau K, Poncet D, Zamzami N, Perfettini JL, Metivier D, Ojcius DM, Jaattela M, Kroemer G. Lysosomal membrane permeabilization induces cell death in a mitochondrion-dependent fashion. J Exp Med. 2003; 197:1323–1334. [PubMed: 12756268]
16. Martinon F. Dangerous liaisons: mitochondrial DNA meets the NLRP3 inflammasome. Immunity. 2012; 36:313–315. [PubMed: 22444626]
17. Nakahira K, Haspel JA, Rathinam VA, Lee SJ, Dolinay T, Lam HC, Englert JA, Rabinovitch M, Cernadas M, Kim HP, Fitzgerald KA, Ryter SW, Choi AM. Autophagy proteins regulate innate immune responses by inhibiting the release of mitochondrial DNA mediated by the NALP3 inflammasome. Nat Immunol. 2011; 12:222–230. [PubMed: 21151103]
18. Shimada K, Crother TR, Karlin J, Dagvadorj J, Chiba N, Chen S, Ramanujan VK, Wolf AJ, Vergnes L, Ojcius DM, Rentsendorj A, Vargas M, Guerrero C, Wang Y, Fitzgerald KA, Underhill DM, Town T, Arditi M. Oxidized mitochondrial DNA activates the NLRP3 inflammasome during apoptosis. Immunity. 2012; 36:401–414. [PubMed: 22342844]
19. Chu J, Thomas LM, Watkins SC, Franchi L, Nunez G, Salter RD. Cholesterol-dependent cytolysins induce rapid release of mature IL-1beta from murine macrophages in a NLRP3 inflammasome and cathepsin B-dependent manner. J Leukoc Biol. 2009; 86:1227–1238. [PubMed: 19675207]
20. Ashley N, Harris D, Poulton J. Detection of mitochondrial DNA depletion in living human cells using PicoGreen staining. Exp Cell Res. 2005; 303:432–446. [PubMed: 15652355]
21. Miao EA, Leaf IA, Treuting PM, Mao DP, Dors M, Sarkar A, Warren SE, Wewers MD, Aderem A. Caspase-1-induced pyroptosis is an innate immune effector mechanism against intracellular bacteria. Nat Immunol. 2010; 11:1136–1142. [PubMed: 21057511]
22. McGuire KA, Barlan AU, Griffin TM, Wiethoff CM. Adenovirus type 5 rupture of lysosomes leads to cathepsin B-dependent mitochondrial stress and production of reactive oxygen species. J Virol. 2011; 85:10806–10813. [PubMed: 21835790]
23. Boya P, Gonzalez-Polo RA, Poncet D, Andreau K, Vieira HL, Roumier T, Perfettini JL, Kroemer G. Mitochondrial membrane permeabilization is a critical step of lysosome-initiated apoptosis induced by hydroxychloroquine. Oncogene. 2003; 22:3927–3936. [PubMed: 12813466]
24. Kroemer G, Jaattela M. Lysosomes and autophagy in cell death control. Nat Rev Cancer. 2005; 5:886–897. [PubMed: 16239905]
25. van Bruggen R, Koker MY, Jansen M, van Houdt M, Roos D, Kuijpers TW, van den Berg TK. Human NLRP3 inflammasome activation is Nox1-4 independent. Blood. 2010; 115:5398–5400. [PubMed: 20407038]
26. Dostert C, Petrilli V, Van Bruggen R, Steele C, Mossman BT, Tschopp J. Innate immune activation through Nalp3 inflammasome sensing of asbestos and silica. Science. 2008; 320:674–677. [PubMed: 18403674]
27. Li Z, Berk M, McIntyre TM, Gores GJ, Feldstein AE. The lysosomal-mitochondrial axis in free fatty acid-induced hepatic lipotoxicity. Hepatology. 2008; 47:1495–1503. [PubMed: 18220271]
28. Misawa T, Takahama M, Kozaki T, Lee H, Zou J, Saitoh T, Akira S. Microtubule-driven spatial arrangement of mitochondria promotes activation of the NLRP3 inflammasome. Nat Immunol. 2013

29. Balint S, Verdeny Vilanova I, Sandoval Alvarez A, Lakadamyali M. Correlative live-cell and superresolution microscopy reveals cargo transport dynamics at microtubule intersections. Proc Natl Acad Sci U S A. 2013; 110:3375–3380. [PubMed: 23401534]

30. Aachoui Y, Leaf IA, Hagar JA, Fontana MF, Campos CG, Zak DE, Tan MH, Cotter PA, Vance RE, Aderem A, Miao EA. Caspase-11 protects against bacteria that escape the vacuole. Science. 2013; 339:975–978. [PubMed: 23348507]

31. Case CL, Kohler LJ, Lima JB, Strowig T, de Zoete MR, Flavell RA, Zamboni DS, Roy CR. Caspase-11 stimulates rapid flagellin-independent pyroptosis in response to Legionella pneumophila. Proc Natl Acad Sci U S A. 2013; 110:1851–1856. [PubMed: 23307811]

32. Shin S, Brodsky IE. Caspase-11: the noncanonical guardian of cytosolic sanctity. Cell Host Microbe. 2013; 13:243–245. [PubMed: 23498948]

33. Zhou R, Yazdi AS, Menu P, Tschopp J. A role for mitochondria in NLRP3 inflammasome activation. Nature. 2011; 469:221–225. [PubMed: 21124315]

34. Hamasaki M, Furuta N, Matsuda A, Nezu A, Yamamoto A, Fujita N, Oomori H, Noda T, Haraguchi T, Hiraoka Y, Amano A, Yoshimori T. Autophagosomes form at ER-mitochondria contact sites. Nature. 2013; 495:389–393. [PubMed: 23455425]

35. Naik E, Dixit VM. Mitochondrial reactive oxygen species drive proinflammatory cytokine production. J Exp Med. 2011; 208:417–420. [PubMed: 21357740]

36. Saitoh T, Fujita N, Jang MH, Uematsu S, Yang BG, Satoh T, Omori H, Noda T, Yamamoto N, Komatsu M, Tanaka K, Kawai T, Tsujimura T, Takeuchi O, Yoshimori T, Akira S. Loss of the autophagy protein Atg16L1 enhances endotoxin-induced IL-1beta production. Nature. 2008; 456:264–268. [PubMed: 18849965]

37. Shi CS, Shenderov K, Huang NN, Kabat J, Abu-Asab M, Fitzgerald KA, Sher A, Kehrl JH. Activation of autophagy by inflammatory signals limits IL-1beta production by targeting ubiquitinated inflammasomes for destruction. Nat Immunol. 2012; 13:255–263. [PubMed: 22286270]

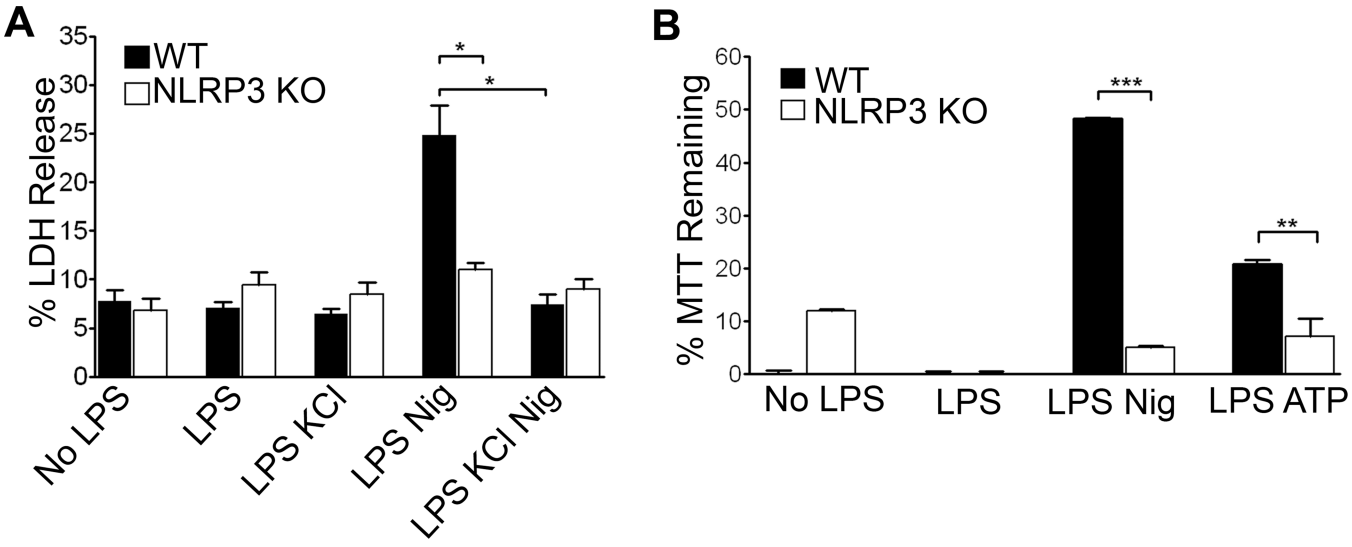

Figure 1. NLRP3 dependent cell membrane damage

(A)LPS primed or unprimed WT and NLRP3$^{-/-}$ BMDM were treated with 20 μM nigericin or 3 mM ATP for thirty minutes with or without KCl. LDH release was recorded as the percent released into the supernatant by five minutes of Triton treatment. LDH assay was allowed to develop for two hours and readings were taken as an average of two wells. Error bars represent mean ± s.d. (n=3, *, P<0.01; LPS Nig WT vs KO: P=0.009; WT LPS Nig vs WT LPS Nig KCl: P=0.004). (B) Conversion of MTT reagent added to cell lysates was measured as absorbance of the colored product formazan. Data were acquired as the percent of absorbance of each well/absorbance of Triton-X treated control cells and graphed as MTT reagent remaining unconverted by mitochondrial reductases. Readings were taken as an average of two wells. Error bars represent mean ± s.d. (n=4, ***, P<0.0001; n=3, **, P=0.0155).

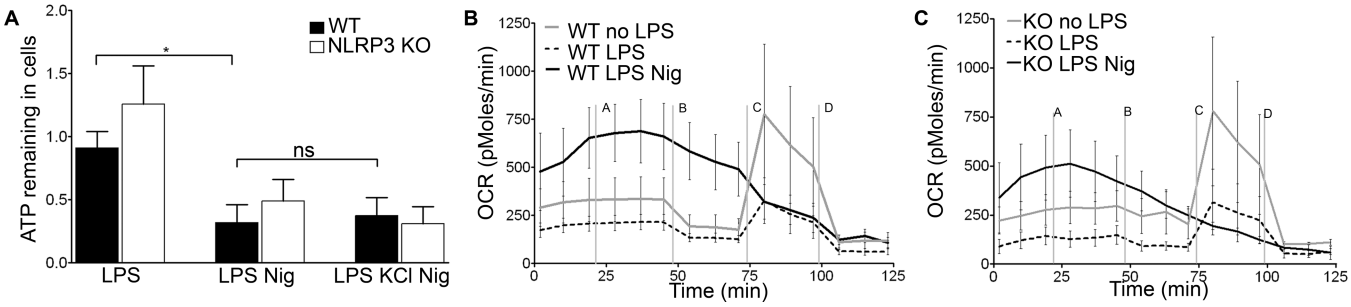

Figure 2. Loss of cellular ATP and decrease in OCR are NLRP3 independent

WT or NLRP3 $^{-/-}$ BMDM were LPS primed and (A) treated with nigericin for thirty minutes with or without KCl. Supernatants were collected and ATP levels measured. Error bars represent ± s.d. (n≥6, *, P=0.0103; ns, p=0.7941) WT BMDM (B) or NLRP3$^{-/-}$ BMDM (C) were treated with nigericin immediately before inserting plate in Seahorse machine. OCR was recorded as an average of 3–4 wells. Media (line a), oligomycin (b), FCCP (c), and rotenone (d) were added as indicated. Error bars represent ± s.d.(n=4, at 45 min, ns, P=0.3099).

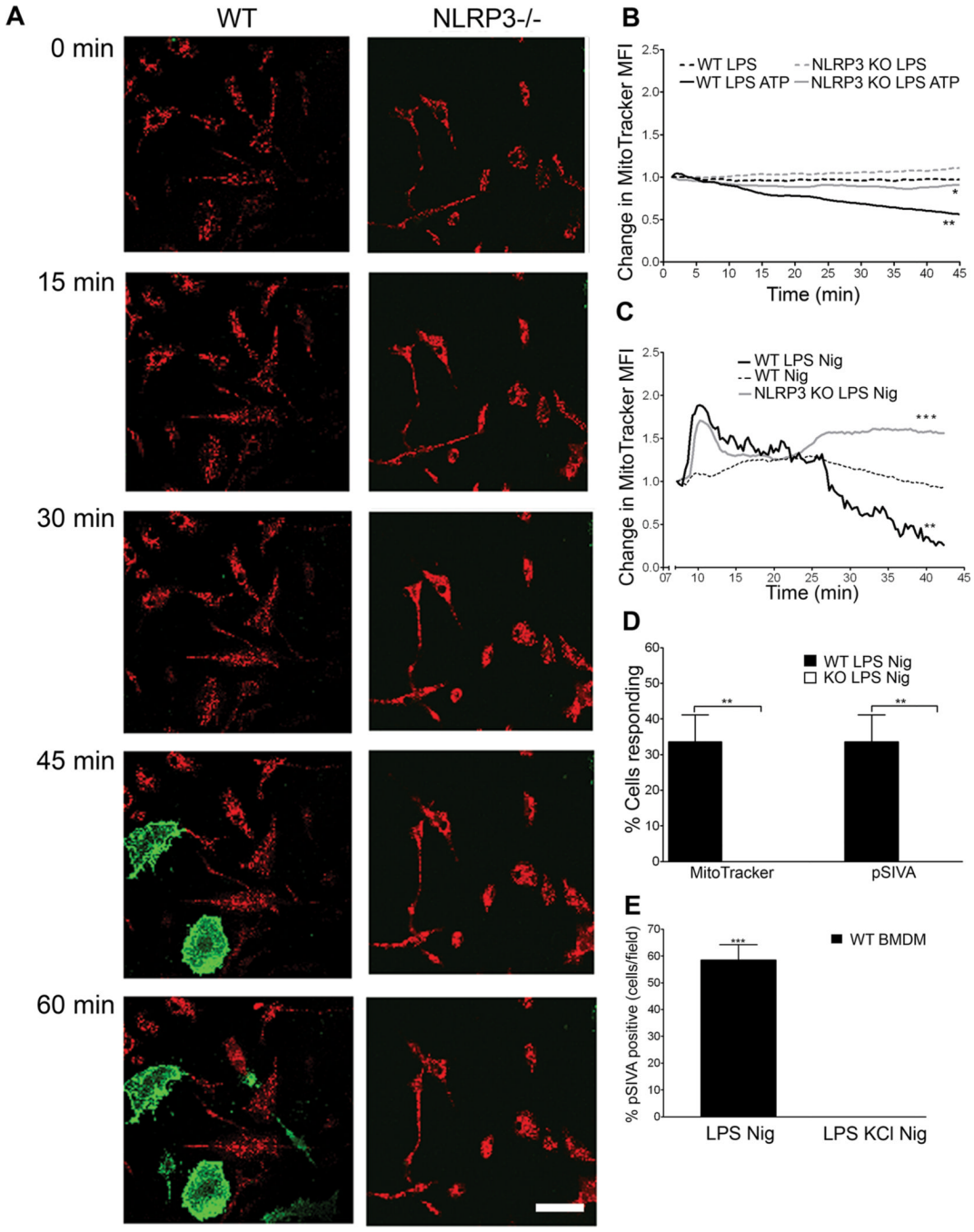

Figure 3. Loss of mitochondrial membrane permeability and cell death are NLRP3 dependent

(A) WT and NLRP3 $^{-/-}$ BMDM were LPS primed and treated with 20 μM nigericin. Cells were stained with MitoTracker red (red) and pSIVA (green), imaged for one hour with a confocal live cell microscope. Images from one representative experiment shown. Scale bar= 50 μm (B) Loss of MitoTracker red signal over time was recorded via live cell microscopy. Cells were left untreated or treated with 3mM ATP. Data was normalized to initial signal with background subtraction. (n≥9, at 45 min *, P=0.0382 for WT LPS ATP vs KO LPS ATP; **, P=0.0021 for WT LPS vs WT LPS ATP). (C) Cells were imaged as in (B) with 20 μM nigericin (n=6; at 40 min. ***, P= 0.0001; **, P=0.0015) (D) Percentage of cells/field that lost MitoTracker signal or gained pSIVA signal over 1 hour of confocal live

cell imaging. Error bars represent ± s.d. (MitoTracker n=4; **, P=0.002; pSIVA, n=3; **, P=0.002) (E) Cells were treated with or without 50 mM KCl and imaged for one hour on a confocal live cell microscope. Percent of cells/field that were pSIVA positive at 60 min recorded. Error bars represent ± s.d. (n=3; ***, P=0.0001).

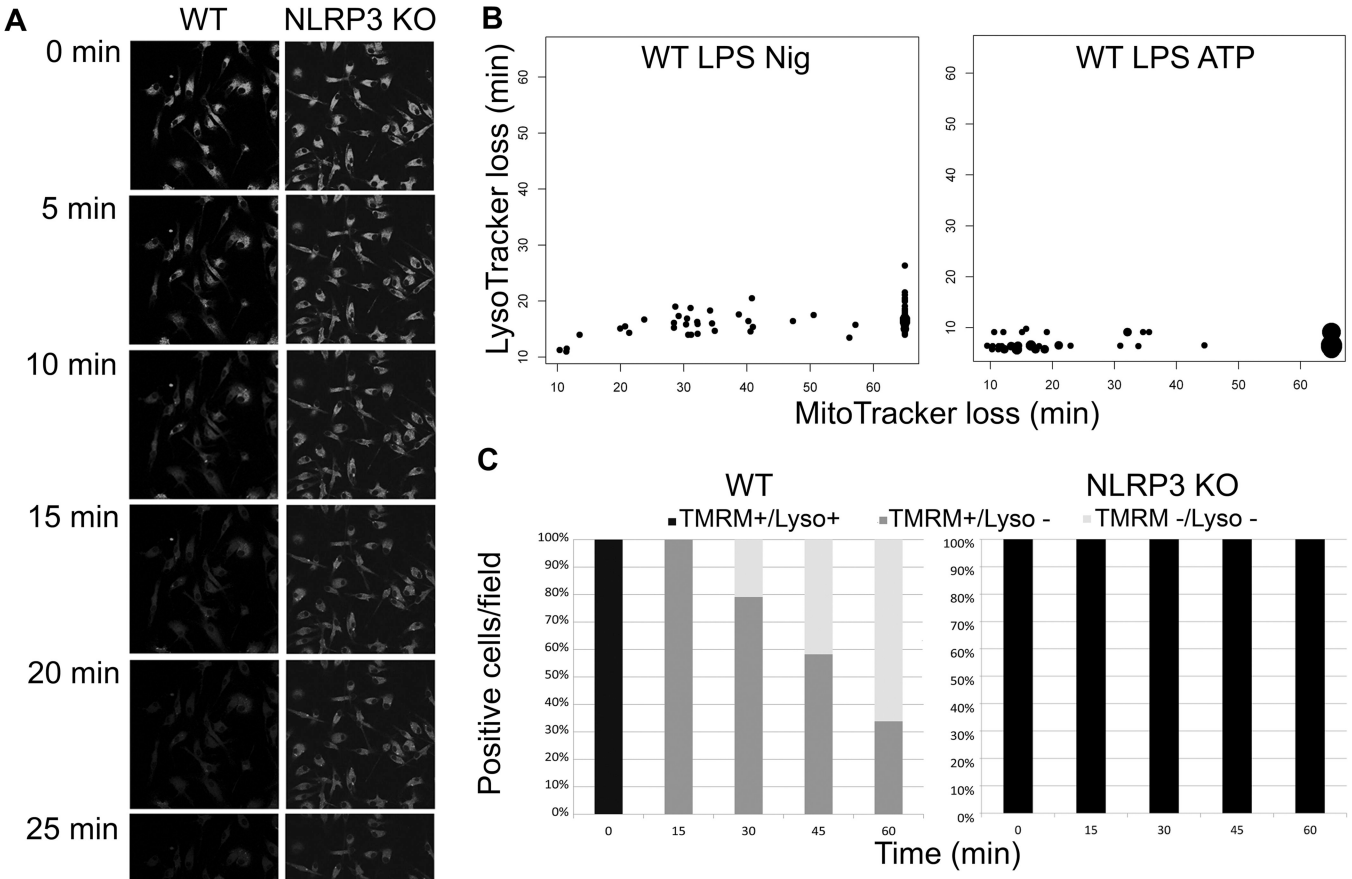

Figure 4. Loss of lysosomal membrane permeability is NLRP3 dependent

(A) WT and NLRP3$^{-/-}$ BMDM were LPS primed, stained with LysoTracker Green and imaged via live cell confocal microscope with 20 μM nigericin treatment for 30 min. Data from one representative experiment shown. Scale bar= 50 μm (B) WT BMDM were LPS primed, treated with 20 μM nigericin or 3 mM ATP, and stained with MitoTracker Red and LysoTracker Green. Cells were imaged for one hour after nigericin or ATP addition via live cell microscopy. Data were recorded as time to loss of signal, each dot represents one cell with larger dots representing multiple cells. Cells that did not lose MitoTracker Red were recorded as data points beyond 60 min imaging period. Data from five fields are displayed. (C) WT BMDM or NLRP3 KO BMDM were LPS primed and nigericin treated, stained with TMRM and LysoTracker Green, and imaged with live cell microscopy for 1 hr. Percent of cells/field staining positive for each of the two dyes was recorded. n≥5 fields.

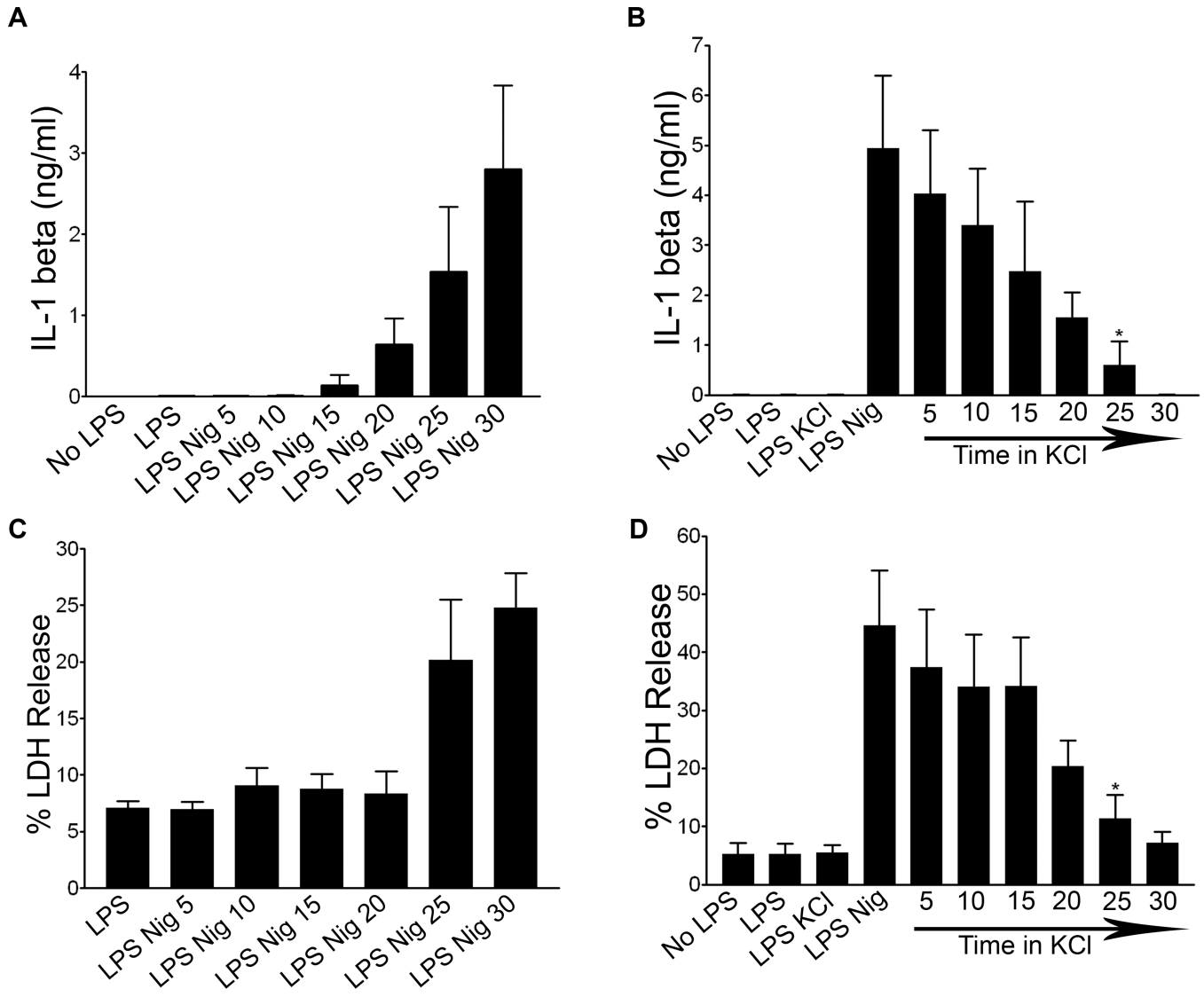

Figure 5. IL-1 beta processing and secretion is kinetically distinct from MMP

WT BMDM were LPS primed or unprimed and (A) treated with 20 μM nigericin for 5–30 minutes. Supernatants were collected and analyzed for IL-1β using ELISA. Error bars represent ± s.d. n=3 (B) WT BMDM were treated with nigericin for thirty minutes. 50 mM KCl was added after 0–25 minutes following nigericin treatment. Supernatants were collected and analyzed via IL-1β ELISA. Error bars represent ± s.d. n≥3 (*, P=0.0294 for LPS Nig KCl 25 vs LPS Nig). (C) WT BMDM were LPS primed and treated with nigericin for 5–30 minutes or (D) were LPS primed and then had 50 mM KCl added 0–25 minutes following nigericin treatment. Supernatants were collected for LDH release analysis. Data shown as percentage of LDH release by Triton-X 100 treated control cells. Error bars represent ± s.d. n=4 (*, P=0.0475 for LPS Nig KCl 25 vs LPS Nig).

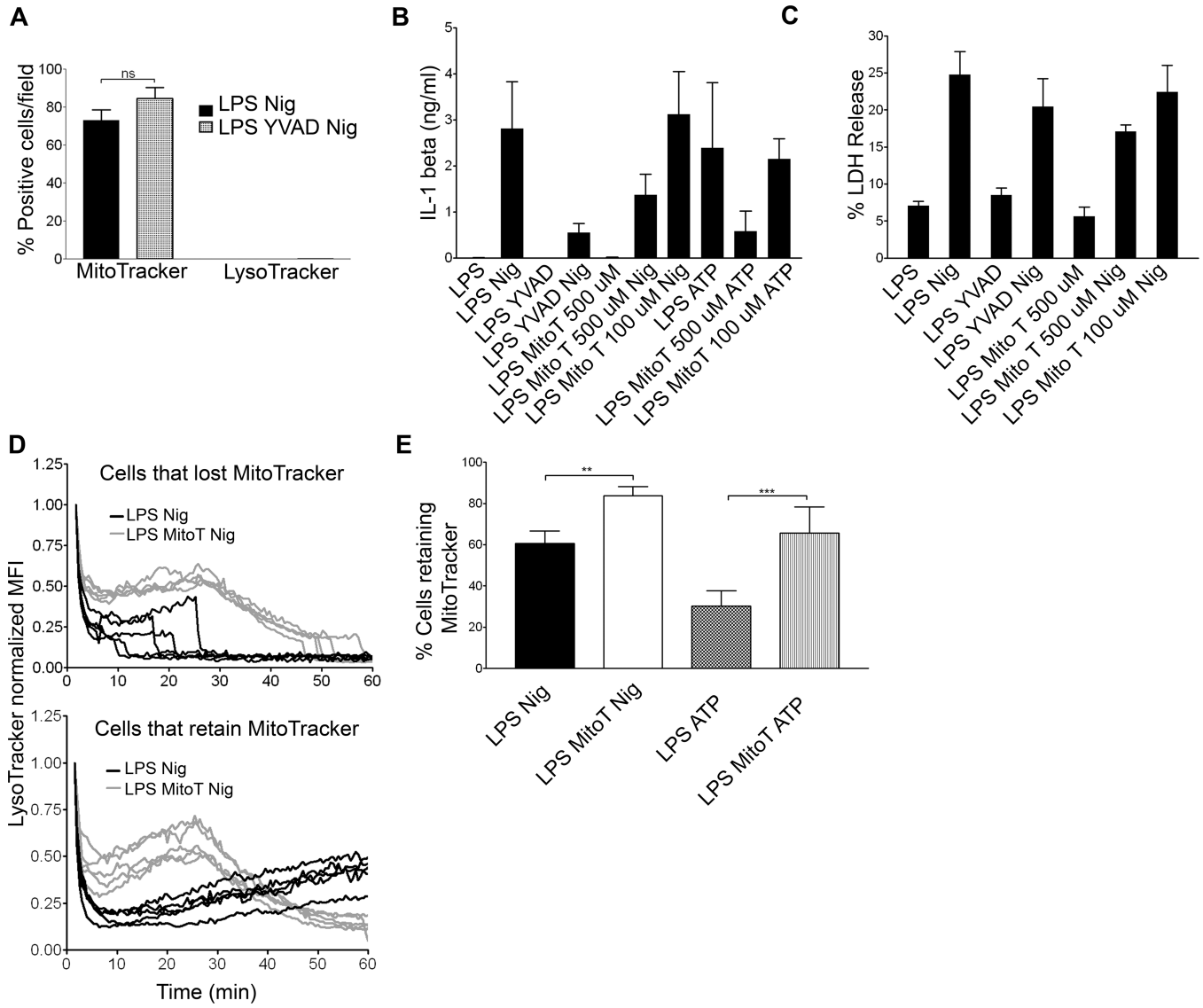

Figure 6. Mitochondrial ROS is required for NLRP3 inflammasome dependent events

(A) WT BMDM were LPS primed, treated with nigericin following YVAD exposure, and labeled with MitoTracker Red and LysoTracker Green. Cells imaged via live cell microscopy for 1 hr. Data presented as positive cells per field at 60 min. Error bars represent ± s.d. n=5. WT BMDM were LPS primed and treated with nigericin following 100 μM YVAD, or 100 μM or 500 μM MitoTEMPO (Mito T). Supernatants were analyzed for (B) IL-1β via ELISA or (C) LDH release as percentage of LDH release by Triton-X 100 treated control cells. Error bars represent ± s.d. n=3 (D) WT BMDM were LPS primed, nigericin and 500 μM MitoTEMPO treated. LysoTracker and MitoTracker (not shown) MFI recorded via live cell microscopy. The LysoTracker MFI was normalized to initial signal and background corrected. LysoTracker data are presented as one line/cell from five representative fields and split into two groups: cells that lost MitoTracker signal after 60 minutes of imaging (top panel) and cells that retained MitoTracker signal throughout the experiment (lower panel). (E) WT BMDM were LPS primed and nigericin or ATP treated with or without 500 μM MitoTEMPO. Cells were labeled with MitoTracker Red and imaged

via live cell microscopy. Data are presented as percent of cells/field retaining MitoTracker signal. Error bars represent ±s.d. n≥ 10 fields. (**, P=0.0061; ***, P< 0.0001).